

# Hydrothermal synthesis of nanostructured MnO<sub>2</sub> under magnetic field for rechargeable lithium batteries

Chao Zhong · Jia-Zhao Wang · Zhen-Zhen Zhu ·  
Shu-Lei Chou · Zhi-Xin Chen · Ying Li · Hua-Kun Liu

Received: 10 November 2009 / Revised: 6 December 2009 / Accepted: 8 December 2009 / Published online: 30 December 2009  
© Springer-Verlag 2009

**Abstract** Nanocrystalline MnO<sub>2</sub> was synthesized by the hydrothermal method with or without pulsed magnetic fields. It was found that the morphology of the MnO<sub>2</sub> prepared without magnetic field has an urchin-like structure, while the MnO<sub>2</sub> prepared with magnetic fields has a rambutan-like structure. A pronounced increase in the Brunauer–Emmett–Teller specific surface area was obtained when the intensities of the pulsed magnetic fields increased. The battery performances were improved for the samples prepared with magnetic fields. The MnO<sub>2</sub> prepared under a magnetic field of 4 T shows a capacity of 121.8 mAh g<sup>-1</sup>, while the MnO<sub>2</sub> prepared without magnetic field only shows 103.0 mAh g<sup>-1</sup> after 30 cycles.

**Keywords** Magnetic field · Nanostructured manganese dioxide · Cathode · Rechargeable lithium batteries

## Introduction

Manganese oxides have porous structures and can be used as cathode materials for lithium batteries [1, 2]. Nanostructured

manganese oxides have demonstrated enhanced electrochemical properties compared to their bulk counterparts [3–5]. It is well known that cathodes with high surface area show better discharge performance and lower degradation rates than cathodes having lower surface areas [6]. Therefore, better electrochemical performance can be expected by adopting various synthesis conditions which can yield high surface area nanostructured materials with different morphologies.

Nanostructured manganese oxides can be prepared through various methods, such as combining the template-based method and sol–gel chemistry [4], the facile wet chemical method [7], and the hydrothermal method [8]. Hydrothermal synthesis has been an interesting technique to prepare materials with different nano-architectures, such as nanowires, nanorods, nanobelts, nanoflowers, and so forth [9–11]. The main advantage of the hydrothermal technique over other soft chemical routes is the ability to control the nanostructures by properly choosing the reaction temperature, time, solvent, and concentrations without any major structure-directing agents or templates. The effects of temperature, time, solvent, and concentration on the morphologies of powders prepared by the hydrothermal method have been extensively studied and reported [11–13]. However, study of the effects of pulsed magnetic field on the morphologies of the resultant powders during hydrothermal synthesis is a new exploration. This is the motivation behind the present work on the synthesis of nanostructured MnO<sub>2</sub> using the hydrothermal method under pulsed magnetic field. The possibility of using this MnO<sub>2</sub> material as cathode for rechargeable lithium batteries is also examined.

## Experimental

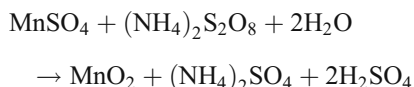
**Manganese dioxide synthesis** Manganese dioxide (MnO<sub>2</sub>) powder was synthesized by the redox hydrothermal method

C. Zhong (✉) · J.-Z. Wang (✉) · S.-L. Chou · H.-K. Liu  
Institute for Superconducting and Electronic Materials and ARC  
Centre of Excellence for Electromaterials Science,  
University of Wollongong,  
Wollongong, NSW 2522, Australia  
e-mail: cz527@uow.edu.au  
e-mail: jiazhao@uow.edu.au

Z.-X. Chen  
School of Mechanical, Materials and Mechatronic Engineering,  
University of Wollongong,  
Wollongong, NSW 2522, Australia

Z.-Z. Zhu · Y. Li  
School of Materials Science and Engineering,  
Shanghai University,  
Shanghai, People's Republic of China

with or without different pulsed magnetic fields. The chemical reaction between  $\text{MnSO}_4$  and  $(\text{NH}_4)_2\text{S}_2\text{O}_8$  is as follows:



All chemical reagents in this work were analytical grade. In a general experiment, 1.082 g (6.4 mmol) manganese sulfate monohydrate ( $\text{MnSO}_4 \cdot \text{H}_2\text{O}$ ) and 1.461 g (6.4 mmol) ammonium persulfate ( $(\text{NH}_4)_2\text{S}_2\text{O}_8$ ) were put into 20 ml distilled water at room temperature to form a homogeneous solution, which was then transferred into a 25-ml Teflon-lined stainless steel autoclave, filling it up to 80% of the whole volume. The sealed solution was kept at 150 °C for 8 h. During this time, different intensities of pulsed magnetic fields (0, 2, and 4 T) were applied respectively. After the autoclave was cooled down to room temperature naturally, the obtained products were then filtered and washed with distilled water to remove the remaining ions. Finally, the as-prepared materials were dried in a vacuum oven at 80 °C overnight.

**Instrumental analyses** X-ray diffraction (XRD) results were obtained using a GBC-MMA-017 X-ray diffractometer with Cu K $\alpha$  radiation ( $\lambda=1.5418 \text{ \AA}$ ). The morphology of samples was investigated by field emission scanning electron microscopy (FE-SEM, JEOL JSM-7500F) and transmission electron microscopy (TEM, JEOL-2011, 200 kV). Energy-dispersive X-ray (EDX) spectroscopy was used for elemental analysis of the materials. To fabricate the  $\text{MnO}_2$  electrodes, 70 wt.%  $\text{MnO}_2$  powder was mixed with 20 wt.% carbon black and 10 wt.% carboxymethyl cellulose binder. De-ionized water was used as the dispersant to form the slurries. The electrochemical characterizations were carried out using CR 2032 coin-type cells, which were assembled in an Ar-filled glove box (Mbraun, Unilab, Germany) by stacking a porous polypropylene separator and a lithium foil counter electrode. The electrolyte used was 1 M LiPF<sub>6</sub> in a 50:50 (v/v) mixture of ethylene carbonate and dimethyl carbonate. The cells were galvanostatically discharged and charged within a voltage window of 2.0–4.0 V (vs. Li/Li<sup>+</sup>) at a current density of 50 mA g<sup>-1</sup> and a temperature of 20 °C. The discharge capacities are based on the amount of active material in the electrodes.

## Results and discussion

Figure 1 shows the XRD patterns of the  $\text{MnO}_2$  materials obtained at 150 °C with (4 T) and without magnetic field.

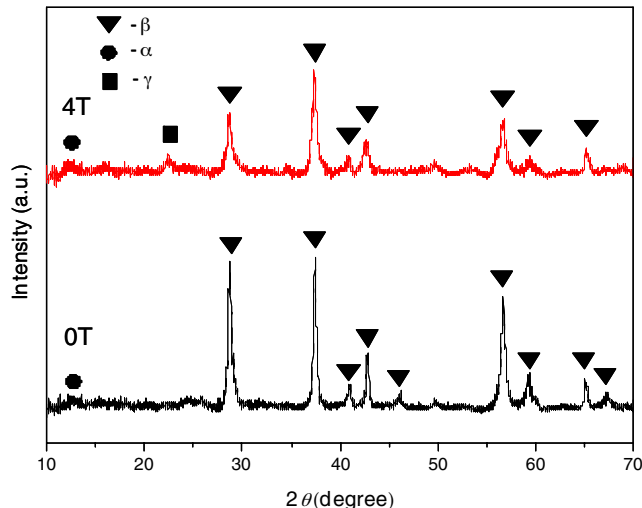


**Fig. 1** XRD pattern of the  $\text{MnO}_2$  obtained without magnetic field and with a 4 T field

All the diffraction peaks correspond well with standard crystallographic data and can be indexed primarily to the pure tetragonal structure of  $\beta\text{-MnO}_2$  (JCPDS card 00-024-0735), but very tiny peaks also correspond to  $\gamma\text{-MnO}_2$  (JCPDS card 00-014-0644) and  $\alpha\text{-MnO}_2$  (JCPDS card 00-044-0141).

Figure 2a–c are FE-SEM images of the  $\text{MnO}_2$  powders synthesized with no magnetic field and with 2 and 4 T pulsed magnetic fields. Comparing the three images, it can be easily seen that the as-prepared  $\text{MnO}_2$  without magnetic field exhibits urchin-like structures which consist of nanofibers about 1  $\mu\text{m}$  in length (Fig. 2a); after using 2 and 4 T pulsed magnetic fields, the morphology of the  $\text{MnO}_2$  changes to rambutan-like structures with longer nanofibers (Fig. 2b and c). From observation of the images we can estimate that the nanofibers for the  $\text{MnO}_2$  obtained at 2 T are approximately 2  $\mu\text{m}$  long. In the material synthesized under a 4 T magnetic field, the nanofibers are even longer than 3  $\mu\text{m}$ . Figure 2d and e are the EDX spectroscopy results for the as-prepared materials obtained at 0 and 4 T magnetic fields. They show that  $\text{MnO}_2$  was the only product, which is consistent with the XRD patterns. The peaks in the region labeled C are from the conductive adhesive.

Figure 3 contains TEM images of the as-prepared  $\text{MnO}_2$  materials obtained in 0 and 4 T magnetic fields. It can be seen that the diameter of the nanofibers prepared with a 4 T magnetic field (10–20 nm) is much smaller than for the sample obtained without magnetic field (40–50 nm). The selected-area electron diffraction (SAED) patterns (inset) display several concentric electron diffraction rings and some regular highlighted diffraction spots on the rings which can be indexed to  $\beta\text{-MnO}_2$ . These results also agree very well with the XRD analysis. The

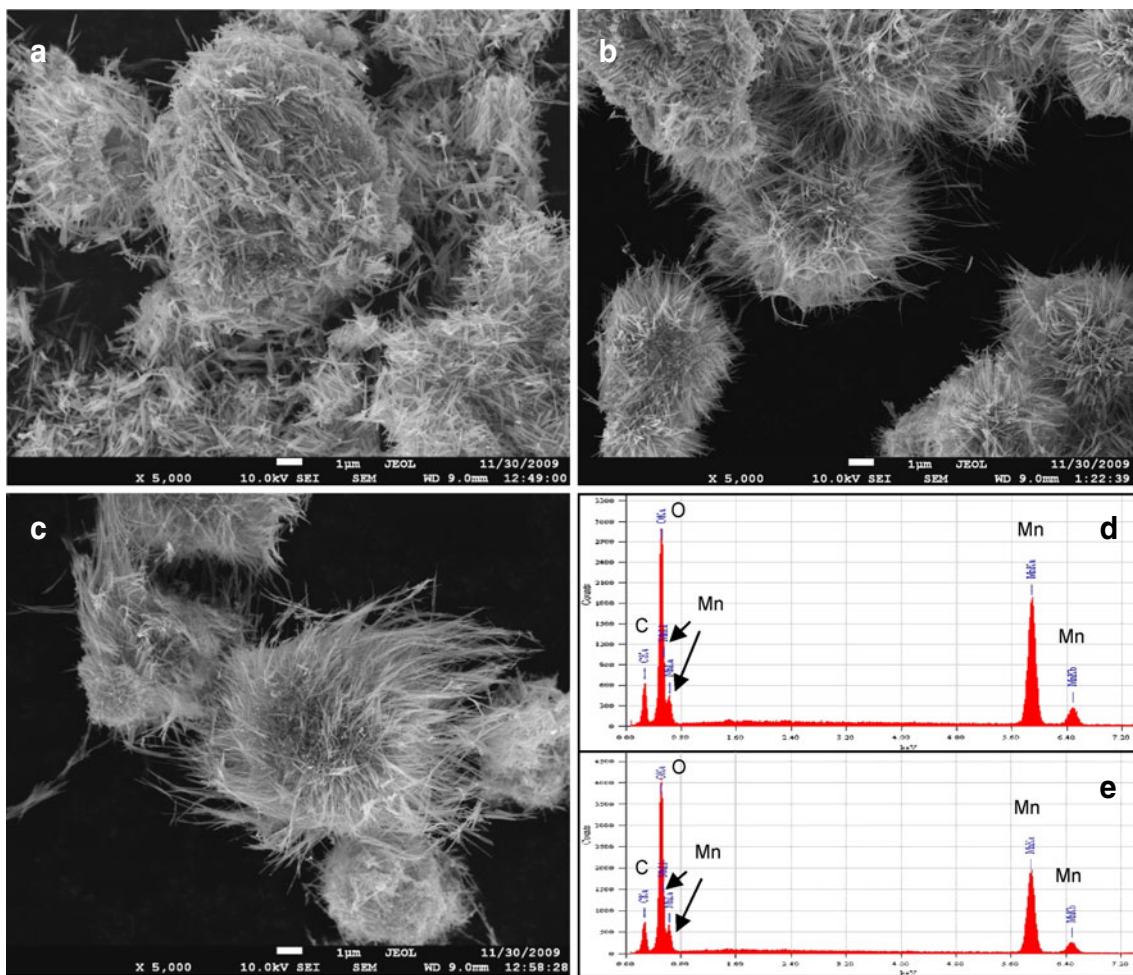


**Fig. 2** SEM images (**a**, **b**, and **c**) for the  $\text{MnO}_2$  obtained without magnetic field, and with 2 and 4 T fields, respectively; EDX results for the  $\text{MnO}_2$  obtained **d** without magnetic field and **e** with a 4 T field

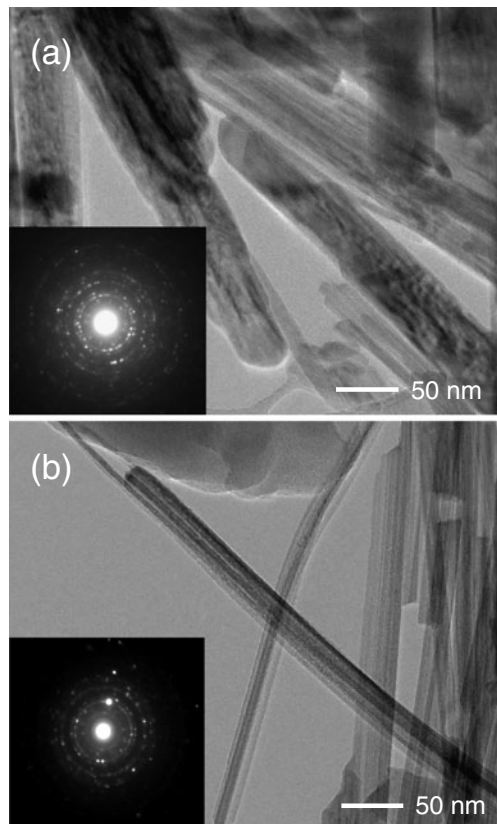
possible reason for the magnetic field effect on the materials is that the magnetic field provides a special directional environment during the hydrothermal process, which affects the nanoparticle nucleation and growth. Thus, the crystals of the  $\text{MnO}_2$  materials follow the magnetic field direction and form narrower and longer fibers. To further study the magnetic field effects on the materials, Brunauer–Emmett–Teller (BET) tests were also performed. The results made it clear that an increase in the intensity of the pulsed magnetic field produced a pronounced increase in the BET specific surface area,  $S_{\text{BET}}$ . The powders obtained from the 2 and 4 T pulsed magnetic fields exhibit the remarkably high  $S_{\text{BET}}$  values of 40.27 and  $46.18 \text{ m}^2 \text{ g}^{-1}$ , respectively, while the sample prepared without magnetic field has a value of only  $23.65 \text{ m}^2 \text{ g}^{-1}$ .

Cyclic voltammograms of the  $\text{MnO}_2$  materials synthesized without magnetic field and with a 4 T pulsed magnetic field at a scan rate of  $0.1 \text{ mV s}^{-1}$  at  $20^\circ\text{C}$  are shown in Fig. 4. During the cathodic and anodic scanning processes, an oxidation potential peak ( $E_O$ ) and a reduction

potential peak ( $E_R$ ) were observed. It can be easily seen that the peak intensities are higher for the sample of  $\text{MnO}_2$  prepared under the 4 T pulsed magnetic field than for the sample of  $\text{MnO}_2$  prepared without magnetic field, which demonstrates that the 4 T synthesized  $\text{MnO}_2$  material has higher reactivity in the lithium cells due to the larger BET specific surface area.

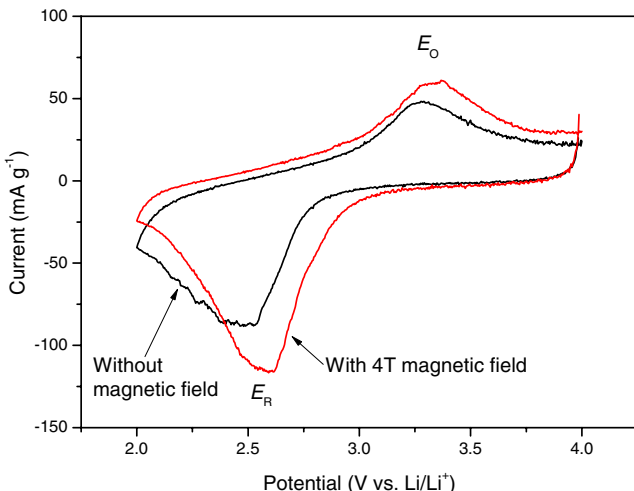
Figure 5a presents the first two typical discharge and charge curves for  $\text{MnO}_2$  materials prepared under different magnetic fields. Comparing the first discharge and charge capacities of the  $\text{MnO}_2$  electrodes synthesized without magnetic field with those synthesized with 2 and 4 T pulsed magnetic fields, it can be found that the irreversible capacity loss for the first cycle is about 27.6% (0 T), 9.8% (2 T), and 2.1% (4 T), respectively. These results show that applying pulsed magnetic fields can greatly help to improve the electrochemical properties of  $\text{MnO}_2$ .

Figure 5b shows the discharge capacity versus cycle number for cells made with  $\text{MnO}_2$  electrodes synthesized



**Fig. 3** TEM images and SAED patterns (*inset*) of the  $\text{MnO}_2$  obtained **a** without magnetic field and **b** with a 4 T field

with and without magnetic fields. It can be observed that the capacity of the electrodes made with  $\text{MnO}_2$  materials synthesized under 4 T pulsed magnetic field ( $121.8 \text{ mAh g}^{-1}$ ) is improved compared to the  $\text{MnO}_2$  synthesized without magnetic field ( $103.0 \text{ mAh g}^{-1}$ ) after 30 cycles. Furthermore, the  $\text{MnO}_2$  synthesized under 4 T pulsed magnetic field gives a



**Fig. 4** Cyclic voltammograms for the  $\text{MnO}_2$  materials synthesized with and without magnetic field

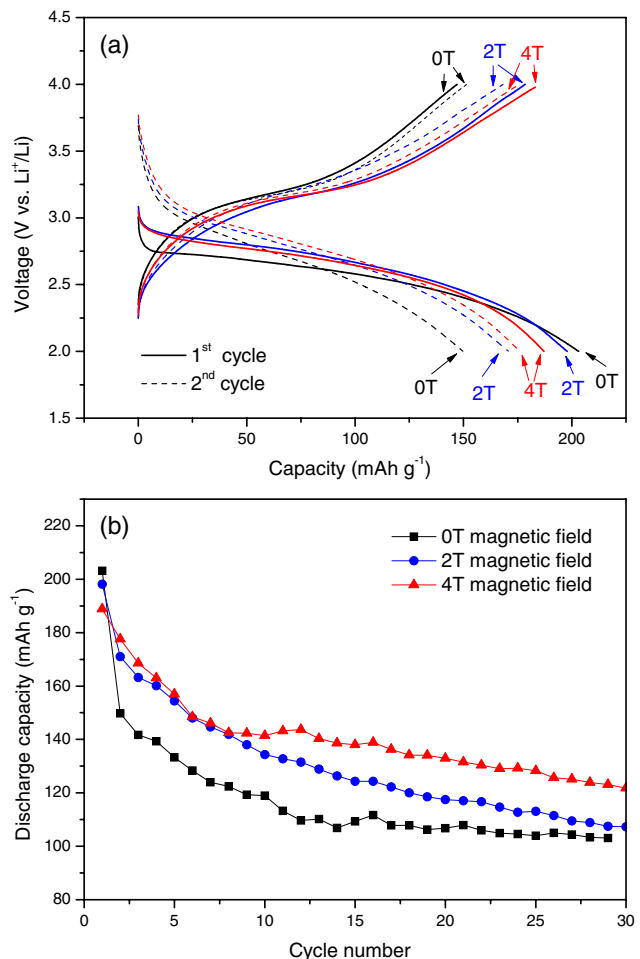


**Fig. 5** **a** Discharge and charge curves for the  $\text{MnO}_2$  materials prepared with different magnetic fields. **b** Discharge capacities vs. cycle number for the as-prepared  $\text{MnO}_2$

better capacity retention of about 64.5% compared to results for the 0 and 2 T materials, which are 50.7% and 54.2%, respectively, beyond 30 cycles. We may conclude that these improvements are due to the special morphologies and the increase in the BET surface areas of the materials. The reactivity of  $\text{MnO}_2$  electrodes with lithium is improved when the samples have larger BET surface areas, as has been reported by Xia's group [14].

## Conclusions

Nanostructured  $\text{MnO}_2$  powders were synthesized by the hydrothermal method under different pulsed magnetic fields, and studied physically and electrochemically in this paper. Magnetic fields have obvious effects on the morphologies of  $\text{MnO}_2$  materials. The BET surface areas of the  $\text{MnO}_2$  materials were increased when the intensities of the magnetic fields increased ( $S_{\text{BET}} 4 > 2 > 0\text{T}$ ). The

electrochemistry results show that the electrochemical performance of the MnO<sub>2</sub> materials was improved with increasing BET surface area.

**Acknowledgments** Financial support provided by the Australian Research Council through ARC Centre of Excellence for Electromaterials Science funding, ARC Discovery Project (DP 0987805) funding, the International Cooperation Program of the Science & Technology Committee of Shanghai Municipality (075207036), and the Program for Changjiang Scholars and Innovative Research Team in University (IRT0739) are gratefully acknowledged. Many thanks also go to Dr. T. Silver for critical reading of the manuscript.

## References

1. Kijima N, Ikeda T, Oikawa K, Izumi F, Yoshimura Y (2004) J Solid State Chem 177:1258–1267
2. Cheng F, Tao Z, Liang J, Chen J (2008) Chem Mater 20:667–681
3. Jiao F, Bruce PG (2007) Adv Mater 19:657–660
4. Sugantha M, Ramakrishnan PA, Hermann AM, Warmsing CP, Ginley DS (2003) Int J Hydrogen Energy 28:597–600
5. Reddy AL, Shajumon MM, Gowda SR, Ajayan PM (2009) Nano Lett 9(3):1002–1006
6. Kunduraci M, Amatucci GG (2006) J Electrochem Soc 153 (7):1345–1352
7. Wang HE, Lu Z, Qian D, Fang S, Zhang J (2008) J Alloy Compd 466:250–257
8. Subramanian V, Zhu HW, Vajtai R, Ajayan PM, Wei BQ (2005) J Phys Chem B 109:20207–20214
9. Du GH, Yuan ZY, Tendeloo GV (2005) Appl Phys Lett 86:063113
10. Wang X, Li Y (2002) Chem Commun 7:764–765
11. Wang JZ, Chou SL, Chew SY, Sun JZ, Forsyth M, MacFarlane DR, Liu HK (2008) Solid State Ionics 179:2379–2382
12. Ellis B, Kan WH, Makahnouk WRM, Nazar LF (2007) J Mater Chem 17:3248–3254
13. Meng Z, Peng Y, Yu W, Qian Y (2002) Mater Chem Phys 74:230–233
14. Luo JY, Zhang JJ, Xia YY (2006) Chem Mater 18:5618–5623